Macromolecular Materials and Engineering
Open Access
www.mame-journal.de

Beyond Yield Optimization: The Impact of Organosolv Process Parameters on Lignin Structure

*Jonas Bergrath, Jessica Rumpf, René Burger, Xuan Tung Do, Michaela Wirtz, and Margit Schulze**

When optimizing the process parameters of the acidic ethanolic organosolv process, the aim is usually to maximize the delignification and/or lignin purity. However, process parameters such as temperature, time, ethanol and catalyst concentration, respectively, can also be used to vary the structural properties of the obtained organosolv lignin, including the molecular weight and the ratio of aliphatic versus phenolic hydroxyl groups, among others. This review particularly focuses on these influencing factors and establishes a trend analysis between the variation of the process parameters and the effect on lignin structure. Especially when larger data sets are available, as for process temperature and time, correlations between the distribution of depolymerization and condensation reactions are found, which allow direct conclusions on the proportion of lignin's structural features, independent of the diversity of the biomass used. The newfound insights gained from this review can be used to tailor organosolv lignins isolated for a specific application.

1. Introduction

The intensive use of fossil resources not only causes permanent damage to the environment, but also its limited availability in the face of growing global demand makes the transition from an oil-based to a bio-based society essential.[1] To meet the enormous demand for industrial goods, renewable resources must be used in all their diversity. In addition, overall concepts for the design of a circular economy are needed. Lignocellulose, as the most abundant renewable resource, offers the greatest potential.[2–4] Full utilization of this material stream requires a process for selective separation into its main components cellulose, hemicellulose, and lignin. Separation, isolation, and subsequent chemical conversion of the three classes of polymers can yield a wide and diverse range of naturally derived chemicals.

One promising approach is the organosolv process, in which lignin and hemicellulose are extracted at elevated temperatures using a mixture of an organic solvent and water.[5] The advantages of this process are the gentle recovery of a very pure lignin fraction and easy recovery of the solvent. In addition, they have great significance for cellulose biorefinery.[6,7] Treatment by organosolv digestion usually results in a significant removal of lignin with minimal loss of cellulose.[8] However, the costly and energy-intensive organosolv step impacts the economics of the cellulose biorefinery process so that the recovery of high-value organosolv lignin does not outweigh the increased cost of the cellulose recovery process.[9]

Lignin, especially in high purity, is considered a valuable feedstock in the currently growing market.[10,11] Although lignin is structurally more complex, its higher carbon and lower oxygen content compared to the cellulose or hemicellulose fraction makes it an attractive feedstock to produce biofuels and chemicals.[12–14] Meanwhile, a structural profile exists for possible lignin applications. Thus, it can be postulated which application the lignin would be suitable for. For example, lignins with high phenolic content could act as antioxidants.[15,16] A lignin with low oxygen content is suitable for producing carbon fibers (for electrodes or supercapacitors), bio-oils, or fillers in hydrophobic composites.[17–19] A high content of aliphatic OH groups in lignin makes it extremely attractive as a feedstock for adsorbents in aqueous systems.[20,21] A lignin with high polydispersity is suitable to produce lubricants or compact lignin nanoparticles,[22–24] while lignins with low polydispersity are excellent for mechanical carbon fibers or hollow lignin nanoparticles.[17,25]

To date, several studies have focused on optimizing delignification, maximizing purity, or idealizing the economic and environmental aspects (circular economy concept) of the organosolv

J. Bergrath, J. Rumpf, R. Burger, X. T. Do, M. Wirtz, M. Schulze
Department of Natural Sciences
Bonn-Rhein-Sieg University of Applied Sciences
von-Liebig-Strasse 20, 53359 Rheinbach, Germany
E-mail: margit.schulze@h-brs.de
J. Bergrath
Department of Chemistry and Biology
University of Wuppertal
42119 Wuppertal, Germany
J. Rumpf, M. Schulze
Faculty of Agriculture
University of Bonn
Meckenheimer Allee 174, 53115 Bonn, Germany

The ORCID identification number(s) for the author(s) of this article can be found under https://doi.org/10.1002/mame.202300093

DOI: 10.1002/mame.202300093

process.[26–29] Often, this is done by varying process parameters via statistical experimental designs and adjusting them for the desired output. In this review however, the focus is on the influence of the most frequently varied process parameters on the chemical structure of the organosolv lignin: most data is available regarding the effect of process temperature and time on the molecular weight, aliphatic and phenolic OH groups, but also the impact of solvent, catalyst, biomass, and additional pre- or post-treatments will be discussed. The focus here is on the most widely used acidic ethanol organosolv process.

2. Organosolv Lignin Structure

Lignin is one of the major constituents of wood and along with cellulose, one of the most abundant natural polymers. Chemically, lignin is a 3D, high-molecular-weight network of phenylpropane units (monolignols) that is formed by dehydrative polymerization and acts as the actual skeletal substance of the plant cell walls. The relative proportions of the three monolignols are characteristic of different plant groups: hardwood lignin contains predominantly sinapyl units (S-units), softwood lignin contains predominantly coniferyl units (G-units), and grass lignin (especially found in straw) has high proportions of coumaryl units (H-units).[30] Pretreatment processes are required to break the covalent bonds between lignin and the carbohydrate fraction and thereby maximize the individual properties of the components of the lignocellulosic biopolymer composite. These processes can be classified as physical, chemical, biological, or a combination of these. So far, kraft, lignosulfonate, and organosolv are the most popular chemical processes, while biological approaches (microbial or enzymatic) are less favored. The kraft process is still the only large-scale pulping process. The principles of the processes and their advantages and disadvantages are described in detail in the literature.[31,32] In recent decades, the focus has been on environmentally friendly biorefinery processes for the full utilization of renewable raw materials and the extraction of lignin with high added value, which is precisely the approach of the organosolv process.[5] Most organic solvents used in the organosolv process are either polar protic or polar aprotic solvents. This results in a cellulose-rich fraction, an organolignin fraction, and a water-soluble fraction containing hemicellulose, acid-soluble lignin, carbohydrate degradation products, organic acids, and other components. Ethanol is the most used solvent for technical approaches such as Alcell pulping or the Lignol process. Some processes use solvents such as acetic acid, 2-methyltetrahydrofuran or γ-valerolactone.[33] Therefore, pulping is carried out in overpressure reactors, most commonly in aqueous ethanol as solvent with acid catalysts like sulfuric or hydrochloric acid.[34] In general, these organosolv processes (also called ethanosolv) are performed at temperatures between 100 °C and 250 °C, whereas the process time varies between 30 and 90 min. Aqueous ethanol concentrations of approximately 30–80 %wt are used for this process.[5,35,36]

To gain a better chemical understanding of the organosolv process, it is necessary to identify the mechanisms of the main reactions taking place in the system. These lead to the degradation of lignin and hemicellulose into lower molecular weight components that are soluble in the used solvent mixture. For this purpose, the possible bonding types of lignin must be considered first. **Figure 1** gives an overview of a schematic organosolv lignin with possible bonding types.

2.1. Depolymerization and Condensation Reactions during the Organosolv Process

The predominant linkages in lignins are the β—O—4'— and α—O—4'—aryl ethers. The distribution of aryl ether bonds in native lignins varies from 35% to 85% depending on the plant species (hardwood, softwood, herbaceous plants) and the exact lignocellulose type of the feedstock.[29,37] Delignification in the organosolv process occurs in three phases.

In the first phase (0—approx. 70 % delignification), C_α—O bonds from α—O—4' structures and C_β—O bonds from β—O—4' structures are hydrolyzed, resulting in a phenolic. However, more modern approaches postulate that α—O—4' linkages are mostly associated with phenylcoumaran and dibenzodioxocin linkages.[38,39] Thus, depolymerization at phenylcoumaran linkages is only effective when both the α—O—4' bond and the C_α—C_β bond are cleaved. Fragmentation of lignin at dibenzodioxocin linkages by cleavage of the α—O—4' and β—O—4' bonds will result in less lignin branching.[40] Cleavage of the unusual or even absent acyclic α—O—4' bonds therefore minimally contributes to the depolymerization of lignin.

The second phase (starting at about 70 % delignification) is determined by the cleavage of the above-mentioned bonds with arylic substituents. **Figure 2** shows the schematic hydrolysis of aryl—ether bonds. At this stage, condensation reactions (formation of C—C bonds) of the lignin degradation products are already taking place.

In the third stage (delignification degree of about 90 %), the ratio of carbohydrate decomposition to delignification increases and condensate formation occurs more frequently. At this stage, delignification is complete. The organosolv process typically results in high-purity lignin with a residual carbohydrate content of approximately < 5 %wt.[34,42–44]

In summary, next to the cleavage of lignin–carbohydrate complexes, the cleavage of C_α—O bonds from α—O—4' structures, and C_β—O bonds from β—O—4' structures is the primary mechanism of the organosolv process.

The remaining β—O—4'-bonds largely determine the reactivity of the isolated organosolv lignin, as they are the most abundant and most reactive bonds and are often the primary target during depolymerization and condensation, as the α—O—4-bonds have already been primarily cleaved during the first delignification stage.[45] This was largely confirmed by the work of Huang et al.[46] They calculated the theoretical bond dissociation energies using density functional theory methods B3P86 at 6-31 G(d,p) level. In the case of the β—O—4' bond, the C_β—O bond with E_B = 209.4 kJ mol^{-1} is significantly lower than the average bond dissociation energy of the C_α—C_β bond with 266 kJ mol^{-1}. The carbon—oxygen bonds of the propyl chains (C_β—O in β—O—4' and C_α—O in α—O—4') of lignin have lower E_B than the carbon—oxygen bonds between aromatics (C_4—O and O—C_5 in 4—O—5' and C_4—O in "α—O—4"). The E_B of the carbon—carbon bonds (C_α—C_β in β"—O—4" and C_α—C_β in β—1') are between the above-mentioned carbon—oxygen bonds. The direct bond between two benzene rings (5–5') has the highest E_B. The

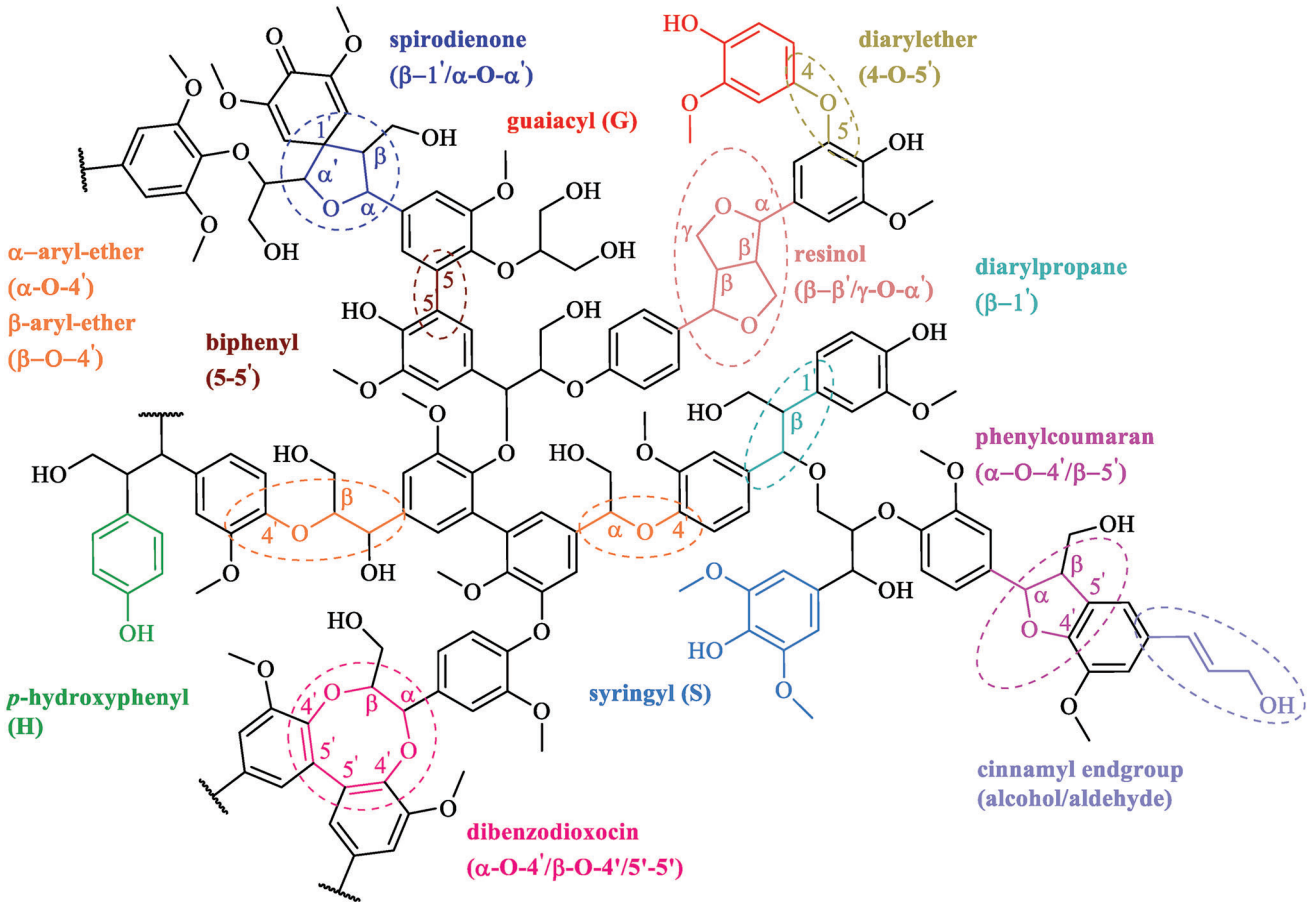

Figure 1. Schematic representation of an organosolv lignin to illustrate the structural building blocks and related linkages; both vary depending on biomass origin and isolation method.

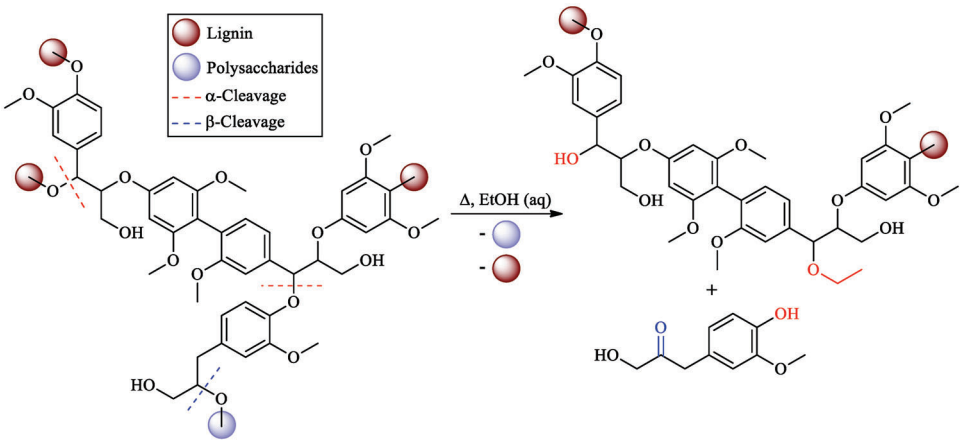

Figure 2. Cleavage of α—ether and β—ether bonds in lignocellulose during ethanol organosolv process. Adapted with permission.[41] Copyrights 2020, Springer Nature.

work of Kim et al. gives comparable results from their M06-2X density functional theory method at the 311++G(d,p) level.[47] Again, the C—C_α, the C_β—C and the corresponding 5—5' biphenyl bond show the highest E_B, whereas the C—O bond within the β—O—4' is much lower (see **Figure 3**).

In addition to theoretical derivations of the bond dissociation energies in lignins, Sturgeon et al. used energy diagrams to calculate the competing mechanisms of depolymerization and condensation in the β—O—4' cleavage.[48] They found that pure lignin condensation has a lower activation energy than both the

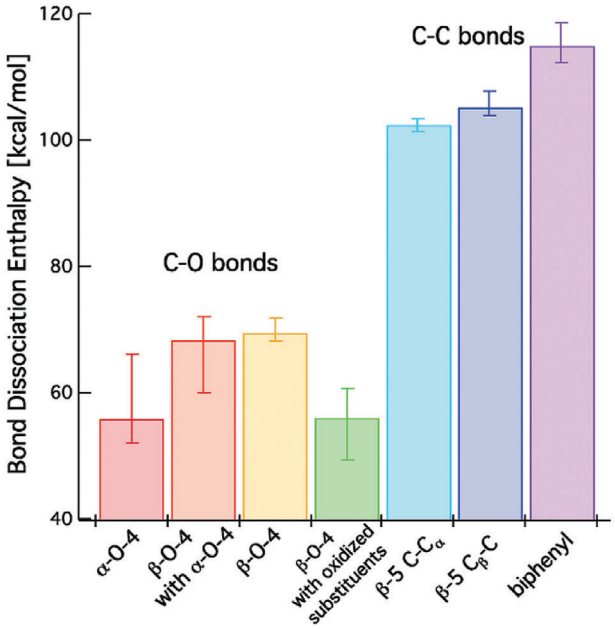

Figure 3. Representative plot of the median considering all calculated derivatives as a function of their substituents. Reproduced with permission.[47] Copyright 2011, American Chemical Society.

corresponding formation of a benzyl cation and lignin hydrolysis, suggesting that lignin condensation proceeds much faster than the competing hydrolysis reaction. The reason why the C—C bonds form so easily under acidic conditions was investigated by Mu et al.[49] They calculated the Gibbs free energy for the condensation reaction between two veratrylglycerol-β-guaiacyl ether lignin model compounds and presented the mechanism of condensation via a benzylic carbocation intermediate and protonation or dehydrogenation transition states. They found that C—C formation is highly exothermic and thus describes the irreversible lignin condensation. Approaches using whole polymers with 10 monomers (G-units) in addition to dimeric and trimeric β—O—4' lignin subunits and calculating conformational states in parallel with bond dissociation energies (BDE) also yielded results in the same order of magnitude.[50] In particular, substituent effects can have a significant influence on the BDE of a β—O—4' bond. For example, oxidation of the α-hydroxyl group to a keto group was found to reduce the BDE by 15 kcal mol^{-1}.[51] The phenylcoumaran linkage contains a five-membered ring resulting from the internal interruption of the intermediate quinone methide by the phenolic hydroxyl group following the β—5' linkage. The ring closure is trans-selective, so there is only one isomer of the dimer. The α—O—4' bonds of the phenylcoumaran exhibit a low computational BDE (about 55 kcal mol^{-1}), indicating that these structural motifs can be easily cleaved by free radicals under very harsh conditions.[40] Regarding the chemical complexity of organosolv lignin, it should be added that there is not one type of β—ether bonds, but different types of structures whose calculated BDE values, depending on the chemical nature of the surrounding S-, G-, and H-units (and other substructures), are in the range of 54–72 kcal mol^{-1}. The results obtained with model compounds must be viewed critically, as the stereochemical influence of the components cannot be considered. In addition to the type of bond, the chemical integration into the cell wall structure also influences the reactivity of the individual bonds.

Some mechanistic approaches to ether cleavage during organosolv process can be formulated. Thus, the C_β—O bond in β—O—4'-structures of organosolv lignin is cleaved under acidic reaction conditions either directly to form a Hibbert ketone and a phenolic derivative (**Figure 4**A1) or to cleave formaldehyde to form an aldehyde and a phenolic derivative (Figure 4A2). The cleavage of the C_α—O bond in α—O—4'-structures is analogous to the cleavage of the β—O—4'-structures, since a Hibbert ketone and a phenolic OH group are formed.[52–54]

During the condensation reactions, new stable C—C bonds (β—β', β—1') are formed whose cleavage is not observed in the organosolv process, while an epimerization of the β—β' linkages is possible.[52] Cyclic α—aryl ether like phenylcoumaran (α—O—4'/β—5') have been shown to be relatively more resistant to degradation during organosolv extraction (see Figure 4B1). Modeling studies of the acidolysis of β—5' structures have shown that the release of formaldehyde can lead to the formation of stilbenes (see Figure 4C).[55]

The released formaldehyde can also initiate another condensation mechanism. The inductive effect of the lignin side chain leads to higher electron densities in its *ortho*- and *para*-position (see **Figure 5**A). Under acidic conditions, both methoxy groups and phenol ether (or free phenol) can also lead to higher electron densities in their *ortho*- and *para*-positions (Figure 5B,C). Therefore, the sum of the inductive effect of the side chain and the resonance effect of the methoxy group leads to higher electron densities at positions 2 and 6 of the aromatic ring.

The electrophilic orientation of the formaldehyde now leads to the formation of a hydroxyl methylene derivative, which forms a methylene bridge in the acidic environment with the intermediary formation of a benzyl cation (see **Figure 6**).[56]

This formaldehyde condensation is pH dependent, as it tends to occur at moderate rates in a slightly acidic range.[57] The coexistence of all these substructures in different equilibrium concentrations leads to a much higher complexity of the system in terms of elucidation of depolymerization or condensation processes.[58]

2.2. Analytical Methods for Lignin Structure Elucidation

An important aspect that should not be neglected are the analytical methods used to determine the structural characteristics since these are not always comparable.

The molecular weight distribution of lignins is usually determined by size exclusion chromatography (SEC) and results are expressed as number-average molecular weight (M_n), weight-average molecular weight (M_w), and polydispersity index (PDI).[59] However, even if SEC is used in most cases, results are not directly comparable, as there are many influencing factors on the outcome of the measurement, like the detector used to determine the retention time (e.g., light scattering, UV absorption, refractive index) or the solvent for lignin dissolution (e.g., sodium hydroxide in water, dimethyl sulfoxide), while tetrahydrofuran is often used for gel permeation chromatography.[60] In addition, the solubility in less polar solvents can be increased by derivatizing the lignin via acetylation, which also has a direct effect on

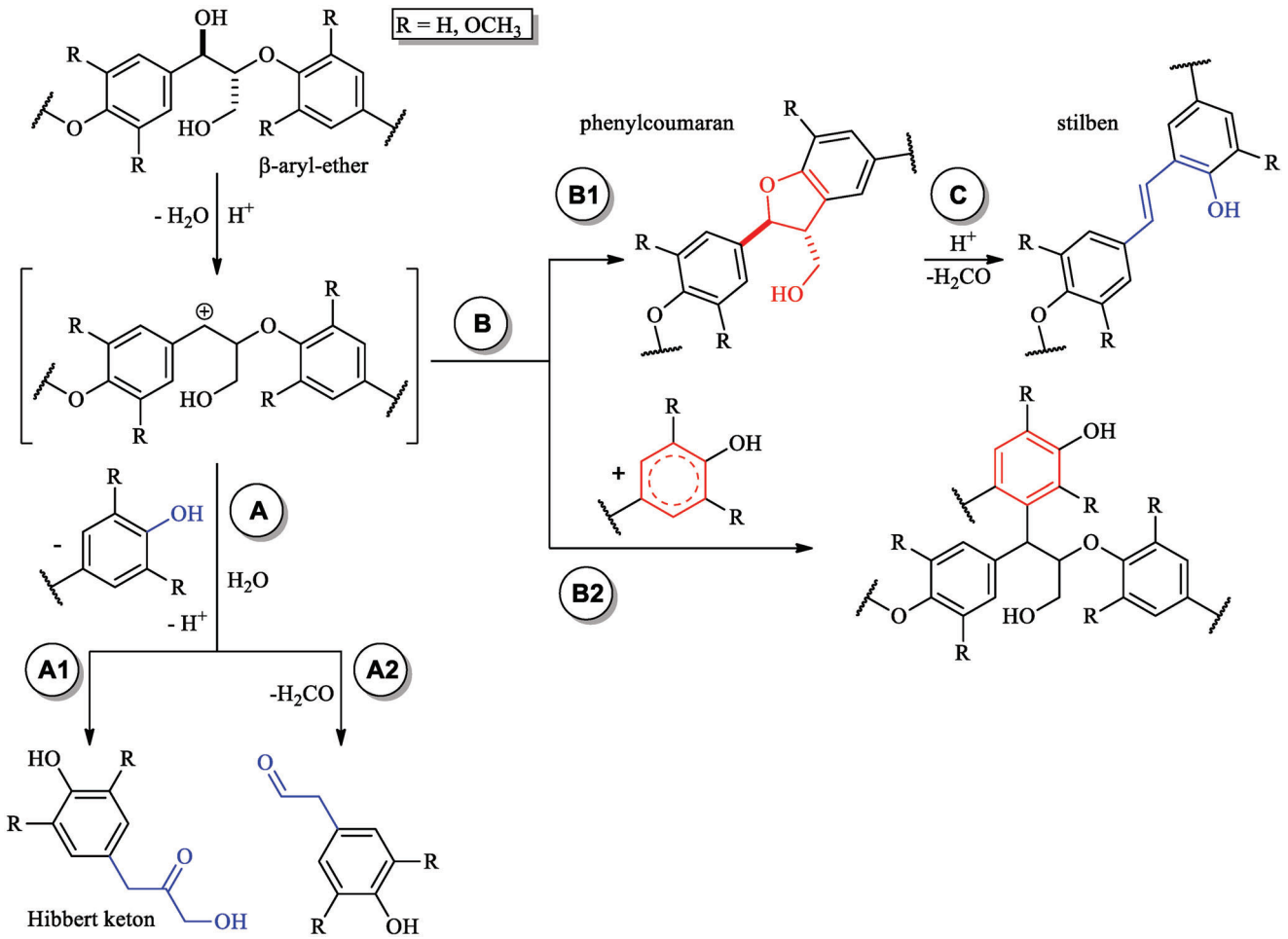

Figure 4. Possible reaction pathways after formation of the α carbocation in the β—O—4' ether A the depolymerization (acidolysis) A1 formation of a ketone (Hibbert ketone) or A2 formation of an aldehyde with cleavage of formaldehyde, B the condensation, where B1 represents the intramolecular phenyl coumaran formation (β—5) and B2 the interchain condensation and C the acidolysis of β—5'-structures.

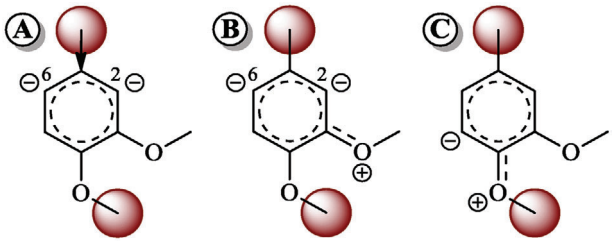

Figure 5. Resonance structures of G-unit at acidic conditions (transferable to other monolignol structures). A) Influence of positive inductive side chain on basic phenolic structure, B,C) Phenolic ether structures result in higher electron density in *ortho* and *para* position.

the weight-average molecular weight.[61] Furthermore, the calibration is mostly performed using polystyrene-based standards, as no lignin molecular weight standards are available, leading to only relative results and no absolute molecular weights.

To quantify the ratio of monolignols, in particular the S/G ratio, techniques such as Fourier transform IR (FT-IR) and 2D NMR spectroscopy, as well as pyrolysis-gas chromatography-mass spectrometry (Py-GC/MS), are used. In FT-IR, semi-quantitative analyses are usually performed on the relative intensities of the specific bands. For this purpose, the aromatic skeletal vibration at approx. 1600 cm^{-1} is often used as a reference band for semi-quantitation of C—H aromatic in-plane deformation vibration of the S-unit (1130–1115 cm^{-1}) or the G-unit (1160–1130 cm^{-1}).[62] NMR experiments can be performed either in one dimension (^{1}H, ^{13}C, ^{31}P) or via 2D heteronuclear correlated recordings (heteronuclear single quantum coherence (HSQC),[63,64] whereby the latter one is used for the semiquantitative determination of monolignol ratios. Pyrolysis is most likely to cleave the aryl—ether linkages (e.g., β—O-4' linkage), forming and detecting their phenolic subunits.[65] Despite the fact that the respective results obtained with these different analytical methods are not comparable in absolute terms, e.g., differences in the amount of monolignols detected by Py-GC/MS versus HSQC NMR,[66] they are sufficient to see relative trends in the lignins examined.

The amount of functional groups can be determined by wet chemical methods such as the Folin—Ciocalteu assay for the determination of the total phenol content (TPC)[27] or a

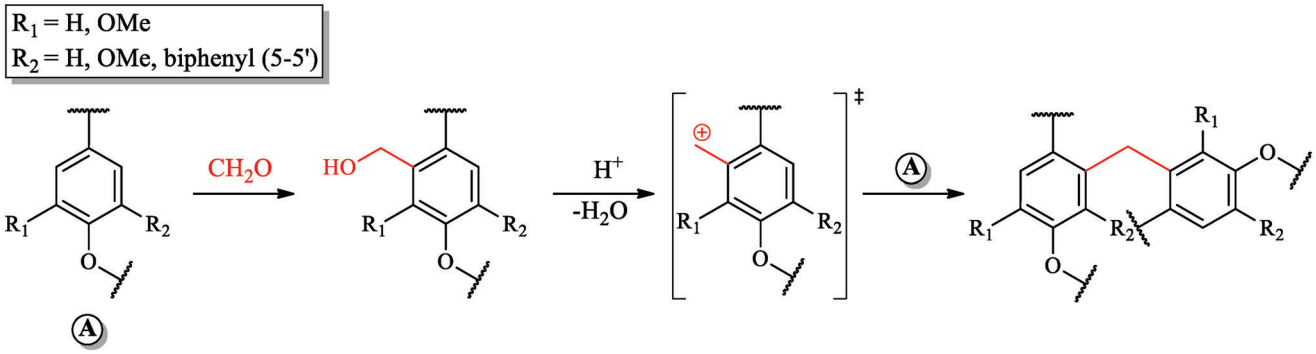

Figure 6. Probable condensation mechanism of monolignol substructures (A) under acidic conditions with in situ formed formaldehyde.

potentiometric titration with tetra-*n*-butylammonium hydroxide for the phenolic OH and carboxylic acid groups.[67] Still, in most cases, spectroscopic methods are used, in particular NMR (^{1}H-, ^{31}P-NMR). Despite the obvious usefulness of NMR spectroscopy for the characterization of lignin, quantitative 2D NMR results should be taken with a grain of salt. While HSQC NMR has the advantage of a good resolution between the various species found in lignins into separate signals, the signal intensity is not inherently quantitative.[68,69] Meanwhile, progress in the quantitative application is consolidating with the use of quick quantitative HSQC (QQ-HSQC) and time-zero HSQC ($HSQC_0$), which use pulse sequences to better quantify the identified substructures. However, semi-quantitative determination of the relative abundance of bonds is possible when the ^{1}H–^{13}C pairs are in a similar chemical environment, such as aliphatic and aromatic agglomeration regions, since one can assume similar $^{1}J_{CH}$ values under these conditions, which lead to a similar response factor.[70,71] Thus, in addition to the monolignol ratios and OH abundances, a statement can be made about the distribution of the various lignin linkages. Burger et al. even address initial approaches to determine the molecular weight of lignins using ^{1}H NMR and multivariate data analysis.[72]

3. Parameters Influencing Organosolv Lignin Structure

The organosolv process has several process parameters that can be varied to control for example delignification or Klason lignin content, but also structural properties like M_w or the proportion of aliphatic and phenolic OH groups, independently of the diversity of a biomass. To identify the impact of individual parameters, this review is limited to acidic ethanosolv processes, as this is by far the prevalent version of organosolv pulping. Still, there are many parameters left including temperature, process time, concentration of solvent and catalyst, solid:liquid ratio, as well as the particle size.

The following chapters deal with the influence of these parameters on the structural characteristics of lignin. For each process parameter with sufficient data, there is a table of relevant studies that performed acidic ethanosolv processes while varying only the discussed parameter. Without the addition of an acid catalyst, the organosolv process is autocatalyzed by released acids.[73] For the optimization of wheat straw organosolv lignin structure, a similar approach has already been already published.[74] The goal is to establish a correlative relationship between "process parameter change ↔ lignin structure".

3.1. Influence of Process Temperature

First, in this section, the effect of a relative increase in process temperature on lignin structure is discussed. The studies that investigated this effect are listed in **Table 1**, showing the used process parameters as well as the resulting lignin characteristics.

Table 1 reflects a clear trend: an increase of the temperature in the organosolv process leads to a decrease of the M_w and M_n and the aliphatic OH groups, while the content of phenolic OH groups increases, among other things, different types of lignocellulosic biomass were used.

In the organosolv process, especially during the second phase of delignification, the lignin structure is altered by a combination of depolymerization and condensation reactions (see **Figure 7**). Depolymerization leads to lignin fragments with smaller molar mass, while condensation leads to lignin fragments with larger molar mass.[78]

Which of these concurrent reactions occur can be a matter of thermodynamic or kinetic control. Theoretical chemical modeling provides evidence for thermodynamic control of the depolymerization reaction and kinetic control of the condensation reaction, since the average bond dissociation energies of the typical condensation products are larger than those of the depolymerization products. Also, the average activation energies of the condensation products are smaller than those of the depolymerization products. Thus, the intermediate, the α-carbocation in the β—O—4' linkage, can condense by kinetic control or depolymerize by thermodynamic control.[84] These findings are in fact supported by experimental observations: While increasing the temperature within a certain range directly increases the amount of depolymerization that takes place. Thus, numerically, the cleavage of the β—O—4' compound (2 aliphatic OH groups) can lead to the formation of a Hibbert ketone (1 aliphatic OH group) and/or a corresponding aldehyde (0 aliphatic OH group). In this process, 1 phenolic derivative is formed. Thus, with increasing degree of depolymerization (increasing temperature), the number of aliphatic OH groups decreases more, and a phenolic group is added. Furthermore, under these harsh process conditions, acid-catalyzed elimination reactions can occur at the corresponding aliphatic hydroxyl groups at any time. In contrast, in the

Table 1. Overview of studies varying the process temperature during organosolv pulping.

Biomass (particle size)	Solvent	Temperature [°C]	Time [min]	Solid:liquid ratio	Catalyst	M_n [Da]	M_w [Da]	PDI	Aliphatic OH [mmol g^{-1}]	Phenolic OH [mmol g^{-1}]	Refs.
Pine Bark (<2 mm)	aqueous ethanol (50 %wt)	150	60	1:10	H_2SO_4 (1 %wt)	2413	7264	3.01	3.23	3.69	[75]
		180				1705	4152	2.44	3.17	4.93	
Hybrid Poplar (*Populus nigra x P.maximowiczii*) (<6.4 mm)	aqueous ethanol (50 %wt)	155	60	1:7	H_2SO_4 (1.25 % wt)	1270	3840	3.02	5.14	2.31	[76]
		180				1075	2089	1.94	3.81	3.39	
		205				994	1579	1.59	3.01	4.24	
Autohydrolyzed poplar (*Populus euramericana*) (ND)	Aqueous ethanol (60 %wt), 1-methylimidazolium chloride	185	180	1:8	Autocatalyzed	1200 ± 8	9300 ± 200	7.75 ± 0.23	ND	ND	[77]
		200				1100 ± 30	7600 ± 400	6.90 ± 0.13			
		215				990 ± 10	4400 ± 40	4.44 ± 0.08			
Soxhlet extracted (toluene/ethanol (2:1)) hybrid poplar (*populus deltoides x trichocarpa*) (0.50–0.355 mm)	aqueous ethanol (65 %wt)	150	330	1:10	Autocatalyzed	700	1900	2.7	3.3 [a)]	3.3 [a)]	[78]
		180				1000	2400	2.4	2.9 [a)]	3.4 [a)]	
		210				900	1500	1.7	1.3 [a)]	3.8 [a)]	
Walnut shell (0.50 –0.30 mm)	ethanol	85	360	1:10	Hydrochloric acid (5 %wt)	4153	15 948	3.84	ND	ND	[79]
		120				3959	13 698	3.46			
Extractive-free *Broussonetia papyrifera* (< 2 mm)	aqueous ethanol (60 %wt)	150	60	1:8	H_2SO_4 (0.45 %wt)	1613	3350	2.08	4.1[a)]	0.86	[80]
		160				1361	2731	2.01	3.6 [a)]	1.3 [a)]	
		170				1308	2782	2.13	3.2 [a)]	1.5 [a)]	
		180				893	1442	1.62	3.0 [a)]	2.12	
larch sawdust (1.5–0.1 mm)	aqueous ethanol (75 %wt)	167	30	1:7	H_2SO_4 (1.10 %wt)	1058	2501	2.36	4.15	3.15	[81]
		177				1117	2403	2.15	3.72	3.50	
		187				970	2022	2.08	3.51	3.91	
Chinese quince fruits (*Chaenomeles sinensis*) (0.425– 0.250 mm)	Aqueous ethanol (60 %wt)	160	90	1:10	Autocatalyzed	3721	11 870	3.19	2.91	2.14	[82]
		200				2255	5636	2.50	1.56	1.95	
		240				1567	2814	1.80	1.15	1.90	
E. globulus (20×25×5 mm)	Aqueous ethanol (50 %wt)	190	75	1:6	Autocatalyzed	1360	4270	3.14	2.577	2.756	[83]
		200				1250	3820	3.06	1.915	3.002	

[a)] Values were taken from figure.

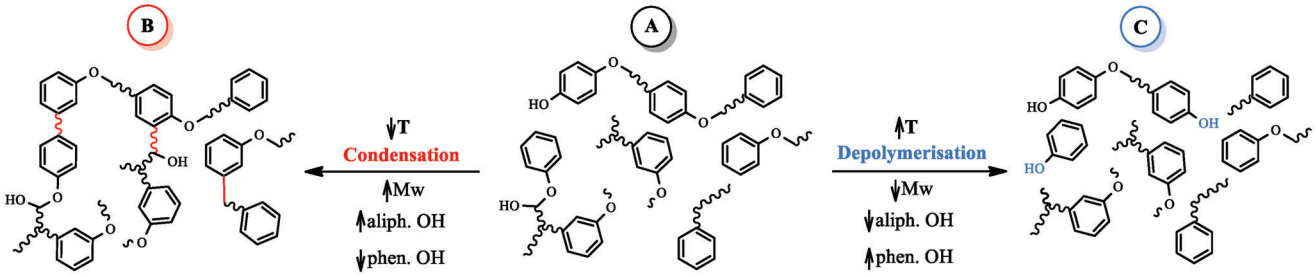

Figure 7. Schematic representation of the influence of temperature on the weight average during the organosolv process. A) organosolv lignin with β—O—4' ether bonds and uncondensed aromatic fragments, B) Condensed C—C bonds and formation of larger polymer chains, C: Cleavage of β—O—4' ether bonds at lower temperatures.

most likely condensation reactions, a maximum of 1 aliphatic OH group is "lost" and no new phenolic subunits are added (see Figure 4).[78,85] This theoretically derived trend is also supported by the experimental work of Ovejero-Pérez et al.[77] They used poplar as biomass and isolated organosolv lignin at different process temperatures (185, 200 and 215°C) and investigated the average molecular weight of the corresponding organosolv lignin structure, which decreased significantly from 9300 ± 200 Da to 7600 ± 400 Da and finally to 4400 ± 40 Da, respectively. The results of this study indicate that the bonds of lignin are cleaved by temperature but not recondensed. They were also able to justify these observations by analyzing their HSQC NMR spectra, where the lignins have higher phenolic contents at the highest temperatures and no recondensation signals in the aromatic region. This temperature-related trend is also observed in the acidic organosolv isolation of lignin from walnut shells. In their work, Nishide et al. investigated various parameters affecting the organosolv process, such as different solvents, catalysts, and process temperatures.[79] They found that in the environment catalyzed by alcoholic acids, an increase in temperature leads to a decrease in polydispersity and average molecular weight. A temperature-dependent trend is also observed by Yao et al.[80] They isolated organosolv lignins from *Broussonetia papyrifera* at 150, 160, 170 and 180 °C, respectively, and examined their structural differences. In addition to the decrease in M_w from 3350 to 1442 Da, the corresponding OH group concentrations also change: the ^{31}P NMR results show both a decrease in aliphatic OH groups and an increase in phenolic OH groups. Again, this phenomenon is attributed to the increasing proportion of β—O—4' bond breaks at higher temperatures.

3.2. Influence of Process Time

The process time of the organosolv pulping also has an influence on the corresponding lignin structure. In this context, **Table 2** presents research that varied the duration of the organosolv process and analyzed average molecular weights, and aliphatic and phenolic OH groups.

As can be seen from Table 2, there is no overall relation between process time and molecular weight, as both an increase and a decrease in the M_w and M_n can be observed. Interestingly, however, we see that similarly to the increase in process temperature, the concentration of aliphatic OH groups decreases with longer process duration, while the concentration of phenolic OH groups increases.

To investigate the influence of process time on the molecular weight distribution of organosolv lignin from hybrid poplar (*Populus deltoides x trichocarpa*), Meyer et al. used SEC to determine these distributions over a period of 25 h at three different temperatures (150 °C, 180 °C, and 210 °C), as can be seen in **Figure 8**.[78]

The data show the influence of process time at different process temperatures. Overall, the molecular weight tends to increase at longer times. This observation is independent of temperature and is probably due to condensation reactions. They also showed that the concentration of aliphatic OH groups decreases and that of phenolic OH groups increases as a function of extraction residence time. Their kinetic model suggests that there are processes that cause aliphatic OH groups to both accumulate and deplete during organosolv extraction, while phenolic OH groups only accumulate. The rate constants of aliphatic OH accumulation are nearly two orders of magnitude lower than the rate constant of degradation, and the apparent activation energies of aliphatic OH accumulation (36 kJ mol^{-1}) are more than twice as high as the apparent activation energy of phenolic OH accumulation (15 kJ mol^{-1}). The observed accumulation of condensed phenolic moieties could result from either 5–5' chain cleavage or 5–5' condensation of two terminal guaiacol moieties. Thoresen et al. also showed that longer treatment times lead to a decrease in aliphatic OH groups, mainly due to a decrease in β—5' structures and a corresponding increase in β—β' structures, indicating the onset of internal condensation.[90] Accumulation of phenolic fragments is likely to be a fundamental and recurring problem in time-dependent trend analysis of acidolysis experiments and may explain the differences (see **Table 3**) when considering M_w.[58] Sturgeon et al. developed modeling approaches for the acidolysis of β—ether bonds in lignin to investigate certain observed differences in the hydrolysis rates of arylic and alkylic dimeric β—ethers. The hydrolysis of alkylic model compounds with aqueous 0.2 M H_2SO_4 solution at 150 °C is about two orders of magnitude slower than the hydrolysis of the corresponding arylic counterpart.[48]

The duration of the acidolysis process should be optimized for each biomass due to the variability of lignin composition to achieve a desired order of magnitude for an average molar mass.[84] Tao et al. isolated lignin from yellow poplar at different times using a mixture of methyl isobutyl ketone, ethanol, and water with H_2SO_4 as a catalyst at 140 °C.[86] Both M_n and M_w decrease on average with time. The M_w of the 30 min lignin

Table 2. Overview of studies varying the process time during organosolv pulping.

Biomass (particle size)	Solvent	Temperature [°C]	Time [min]	Solid:liquid ratio	Catalyst	M_n [Da]	M_w [Da]	PDI	Aliphatic OH [mmol g^{-1}]	Phenolic OH [mmol g^{-1}]	Refs.
E. globulus (20×25×5 mm)	Aqueous ethanol (50 %wt)	200	50	1:6	Autocatalyzed	1240	3490	2.81	1.985	2.981	[83]
			75			1250	3820	3.06	1.915	3.002	
Liriodendron tulipifera (20×20×5 mm)	MIBK, ethanol, water (16/34/50 % wt)	140	30	1:14	H_2SO_4 (0.05 M)	1800	8300	4.6	3.41	1.69	[86]
			45			2000	8300	4.2	2.80	2.33	
			60			1400	6000	4.3	2.70	2.77	
			75			1800	6900	3.8	2.52	3.02	
			90			1300	7100	5.5	2.58	2.82	
			105			900	5900	6.6	2.27	3.24	
			120			1400	5700	4.1	2.05	3.52	
Soxhlet extracted (toluene) Walnut shells (<2 mm)	aqueous ethanol (80 %wt)	80	15	1:10	HCl (0.24 M)	640	831	1.30	ND	ND	[54]
			60			887	1577	1.78			
			180			1013	1782	1.76			
Soxhlet extracted (toluene/ethanol (2:1)) hybrid poplar (*populus deltoides x trichocarpa*) (0.50– 0.355 mm)	aqueous ethanol (65 %wt)	210	15	1:10	Autocatalyzed	1300	3500	2.7	3.8 [a)]	2.0 [a)]	[78]
			60			1100	2300	2.1	2.5 [a)]	3.1 [a)]	
			150			800	1200	1.6	1.8 [a)]	3.7 [a)]	
			330			900	1500	1.7	1.3 [a)]	3.8 [a)]	
			720			900	1600	1.7	0.8 [a)]	3.9 [a)]	
			1500			700	1200	1.6	1.0 [a)]	4.6 [a)]	
Hybrid Poplar (*Populus nigra x P. maximowiczii*) (< 6.4 mm)	Aqueous ethanol (50 %wt)	180	25	1:7	H_2SO_4 (1.25 %wt)	1167	2953	2.53	4.67	2.86	[76]
			60			1230	3100	2.52	4.49	2.80	
			95			1087	1942	1.79	3.78	3.55	
Soxhlet extracted (toluene/ethanol (2:1)) *Broussonetia papyrifera* (2 mm)	Aqueous ethanol (50 %wt)	160	5	1:10	H_2SO_4 (0.05 M)	2569	8567	3.34	3.89	0.62	[87]
			10			2466	9229	3.74	4.21	0.54	
			60			3478	13 882	3.99	3.56	0.47	
Populus tomentosa (40×40×20 mm)	aqueous ethanol (60 %wt)	205	0	1:10	Autocatalyzed	5370	9380	1.75	3.55	1.85	[88]
			30			4750	8310	1.75	2.69	2.20	
			60			4030	6800	1.69	2.17	2.49	
			90			3650	5880	1.61	1.88	2.69	
			120			3480	5400	1.55	1.69	2.62	
			150			3220	5070	1.58	1.64	2.72	
Miscanthus giganteus (< 2 mm)	Aqueous ethanol (95 %wt)	Reflux	120	1:9	HCl (0.02 M)	1350	2210	1.64	ND	ND	[89]
			240			1240	2250	1.81			
			480			1170	2380	2.03			
Wheat straw (< 10 mm)	Aqueous ethanol (60 %wt)	190	90	1:10	Autocatalyzed	ND	ND	ND	2.04	2.45	[74]
			120						1.88	2.55	

[a)] Values were taken from figure.

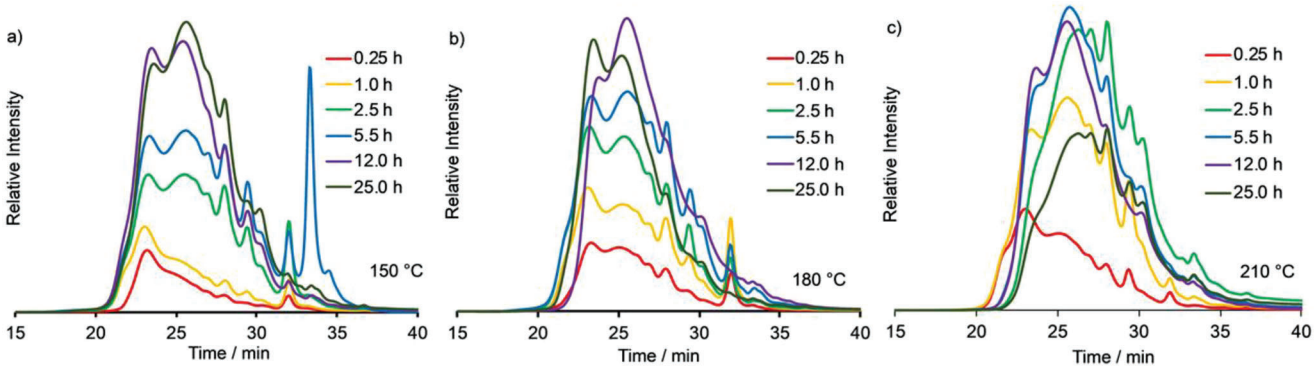

Figure 8. The SEC chromatograms of ethanol organosolv lignins isolated after different process times (0.25—25.0 h) at a) 150 °C, b) 180 °C and c) 210 °C. Reproduced with permission.[78] Copyright 2020, Wiley-VCH GmbH.

is the highest of all fractions, possibly due to minimal depolymerization and side reactions of the lignins in the early stages of the organosolv reaction. With longer durations, the aliphatic OH decreases, while the phenolic OH concentration in the lignin fractions increases. They also explained this observation with the acid-catalyzed elimination of aliphatic OH and the simultaneous formation of new phenolic OH via β—aryl ether bonds.

3.3. Influence of Other Process Parameters

3.3.1. Catalysts

The use and concentration of catalysts such as hydrochloric acid, sulfuric acid, formic acid, or acetic acid in the organosolv process not only affects delignification,[91] but can also have an impact on the chemical structure of the isolated lignins. Higher acid concentrations homogeneously catalyze the hydrolytic cleavage reactions, especially of the β—O—aryl bonds.[92] However, the addition of acid can also accelerate undesirable reactions, such as condensation of the products.[93] The acid concentration to be used is therefore a matter of optimization. There are also approaches using Lewis acids, like aluminum chloride and iron(III) chloride, but these still have ecological and economic disadvantages.[94] Without the addition of an acid catalyst, the organosolv process is autocatalyzed by the release of an organic acid, mainly acetic acid, from hemicellulose components such as O-acetyl-4-O-methylglucoronxylan or glucomannan.[73] In this process, the deacetylation of the hemicelluloses is sufficient to lower the pH from 7 to about 4, which initiates the acid-catalyzed solvolysis of the most unstable β—aryl—ether bonds.[95]

The influence of the addition of 0.5 M HCl compared to the autocatalyzed process on lignin's structure was investigated by Leskinen et al.:[96] the distribution of the chemical substructures of the isolated lignins did not change, while the M_w decreased significantly in the acid-catalyzed process. This suggests that the addition of HCl facilitates hydrolysis reactions which lead to the depolymerization of some otherwise insoluble high molecular weight lignins.

A similar observation was made by Huijgen et al.:[74] they isolated lignins at 190 °C after 1 h in 60 % aqueous ethanol, and added different concentrations of H_2SO_4 (0×10^{-3}, 15×10^{-3}, and 30×10^{-3} M, respectively) to examine the structural changes in the resulting lignins. They used ^{31}P-NMR as well as a wet chemical method to determine the aliphatic and phenolic OH content, resulting in no clear correlation with acid concentration. In fact, they were able to show that with the wet chemical method used,[97] the content of aliphatic OH groups is minimal at 15×10^{-3} M H_2SO_4, whereas with ^{31}P-NMR a maximum occurs at this acid concentration. In addition, also no effect of the acid on the molar mass distribution was found. These inconsistent results make it unclear how the addition of sulfuric acid as a catalyst affects the lignin structure and its functional groups present.

3.3.2. Ethanol Concentration

The concentration of the solvent used, usually ethanol, also affects the resulting organosolv lignin. Early yield-oriented work has shown that the use of mixtures of organic solvents and water results in more effective delignification of the lignocellulose compared to pure solvents, since it combines the advantages of both components. The use of water only results in the extraction of hemicellulose, leaving the lignin content in the wood.[98,99] In order to achieve better delignification, it is necessary that the mixture of organic solvent and water has a Hildebrand parameter of about 25 MPa, which corresponds to the solvent parameter of lignin.[100] The mixture of organic solvent and water should facilitate the soaking of the plant tissue and the transport of the soluble lignin fragments from the matrix to the digestion solution.[101] Thus, lignin and hemicellulose can be selectively dissolved from the lignocellulosic composite while the cellulose fraction remains. Good solubility promotes lignin solvolysis and results in a reduction of lignin condensation reactions.[102] An increasing lignin solubility with increasing ethanol content (0–40% wt) has been observed experimentally.[103] In addition to the technical advantages and disadvantages of varying ethanol concentration, there are also some approaches that describe the influence on the structural composition of lignin. According to experimental work, the influence of an increase in ethanol concentration is often accompanied by a decrease in M_w. However, the content of aliphatic and phenolic OH groups is likely to behave very differently.

Table 3. Comparison of organosolv lignins isolated from untreated biomass versus autohydrolyzed biomass.

Biomass (particle size)	Autohydrolysis parameters	Organosolv parameters	M_n [Da]	M_w [Da]	PDI [-]	S/G ratio [-]	Aliph. OH [mmol g^{-1}]	Phen. OH [mmol g^{-1}]	COOH [mmol g^{-1}]	Refs.
Eucommia ulmoides Oliver wood (20–40 mesh)	–	180 °C, 30 min, 50% aq. EtOH with 1% HCl, 1+10 (w+v)	270	1090	4.0	4.16	0.70	3.27 (2.11 S, 1.16 G)	0.18	[120]
	180 °C, 30 min, 10% solid loading		900	1770	2.0	3.70	0.42	3.12 (2.05 S, 1.07 G)	0.09	
Ziziphus lotus (< 5 mm)	–	180 °C, 60 min, 60% aq. EtOH without catalyst, 1:10 (w/w)	1255	6082	4.85	1.57	–	–	–	[121]
	190 °C, 1:8, s_0 = 3.39		753	2418	3.21	1.93	–	–	–	
Almond shells (1–2 mm)	–	200 °C, 90 min, 70% aq. EtOH without catalyst, 1:6	1072	8301	7.8	Increase in S/G ratio observed for double-step process	–	15.6	–	[122]
	179 °C, 23 min, 1:8		1520	9020	5.9		–	26.2	–	
Walnut shells (1–2 mm)	–		1246	6371	5.1		–	16.5	–	
	200 °C, 1:8		1359	7644	5.6		–	27.2	–	
Beechwood (2.5– 3.5 mm)	–	155 °C, 160 min, 50% aq. EtOH with 100 × 10^{-3} M H_2SO_4, 1:4 (s:l)	891	2607	2.9	–	–	1.8[a)]	0.6[a)]	[123]
	175 °C, 60 min, 1:4		1177	3163	2.7	–	–	1.3[a)]	0.45[a)]	
Miscanthus (1– 3 mm for AH, 200 µm for OS)	–	150 °C, 60 min, 80% aq. EtOH with 0.5 w/w H_2SO_4, 1:8	1932	5715	2.96	–	1.73	0.91 (0.28 S, 0.38 G, 0.25 H)	0.02	[124]
	150 °C, 480 min, 1:9		1496	5103	3.41	–	0.94	1.37 (0.55 S, 0.53 G, 0.29 H)	0.07	
Bamboo (20– 40 mesh)	–	107 °C, 180 min, formic acid/acetic acid/water (30/50/20, v/v/v), 1:20 (w:v)	1490	2540	1.71	2.5	2.44	1.37 (0.72 S, 0.51 G, 0.14 H)	0.05	[125]
	180 °C, 30 min, 10% solid loading		1220	2780	2.27	4.4	1.02	2.49 (1.50 S, 0.75 G, 0.24 H)	0.15	

[a)] Values were taken from figure.

In a batch experiment, Zijlstra et al. investigated the effect of increasing the ethanol concentration by isolating lignin from walnut shells at 120 °C for 5 h with 0.18 M H_2SO_4 using 50 %wt, 80 %wt,and 95 %wt, aqueous ethanol.[104] In addition to the decrease in M_n and M_w, a decrease in β—O—4' bonds from 38 to 28 and 10 per 100 C9 units, respectively, was observed using 2D-HSQC NMR, next to a parallel increase in condensed S-units. Paulsen et al. also performed organosolv extractions with different ethanol concentrations.[90] The extraction with the highest ethanol content (70 %wt) resulted in lignin characterized by a low PDI. Similarly, the lignin is characterized by an extremely low content of β—O—4' linkages and a tendency toward a lower content of condensed aliphatic β—β' and β—5' structures.[105] This is justified by a higher total $S_{2,6}$ + G_2 aromatic content with more S than G units, making the lignin more likely to have unoxidized/condensed aliphatic linkages and thus more condensed/oxidized aromatic structures. This explanation is supported by the relatively high proportion of aliphatic OH groups. The lignin extracted with 50 %wt aqueous ethanol (medium concentration range) is characterized by the dominant presence of β—O—4' units, the presence of aliphatic condensate structures such as β—β' and β—5' and cinnamate end groups. The average molecular weight showed a maximum. However, it should be noted that the presence of xylan residues in the HSQC spectrum should be considered as a procedural drawback.

3.3.3. Particle Size of the Biomass and Solid to Liquid Ratio

In addition to the above-mentioned process parameters, there are also possibilities to influence the organosolv process via the particle size of the biomass used or via the solid/liquid ratio used. Both parameters are highly process-engineered and primarily serve to maximize lignin yield. Particle size adjustment impacts specific particle size distributions and particle shapes, the surface area, as well as physical and chemical material properties. Most commonly, lignocellulosic materials are ground to a particle size of 0.1–15 mm. The choice of particle size is rather arbitrary, mostly depending on the available mill.[26] Particle size reduction is not always an effective way to increase the yield of organosolv lignin, as shown by Wildschut et al.[91] To date, only a few studies have investigated the change in lignin structure as a function of the biomass particle size used. However, some experimental work has shown that decreasing particle size not only results in higher lignin yields,[106] but also affects the lignin's chemical structure. Rumpf et al. presented a comparative study of organosolv lignin from *Miscanthus x giganteus* and *Paulownia tomentosa* with particle sizes of 1.6–2.0 mm, 0.5–1.0 mm, and <0.25 mm, respectively, resulting in a higher M_w at a smaller biomass particle size.[42] There are mechanochemical explanations for this behavior of the average molar mass. For example, Zhu et al. postulated a possible homolytic cleavage of β—O—4'-bonds.[107] Subsequent recombination and/or free radical chemistry of the phenoxy radicals or the β-radical could lead to a larger average molar mass. At this point, we would like to suggest that for future organosolv processes of lignocellulosic biomass, not only the particle size (mesh size), but also a granulometric characterization of the samples used should be reported. By providing a particle size distribution, the influence of different particle sizes on the corresponding lignin structure could be more accurately compared with other organosolv processes. This is because comminution depends primarily on the material anatomy and the mill used.[108] Therefore, "smaller than" specifications are usually too unspecific, as the granulometric distribution may still be different.[109]

The solid:liquid ratio is a very practical process parameter. The choice of ratio is not primarily based on optimizing delignification, but on the solvent absorbency of the biomass and the process conditions.[110] Factors such as reactor geometry, agitator, or solvent absorbency of the biomass used, justify the selection. Commonly used solid:liquid ratios are in the range of 1:4–1:10.[36,92] The influence of the solid:liquid ratio on the corresponding lignin structure is not deeply investigated. organosolv lignin from pine bark and oak bark, respectively, was isolated by Liu et al. at different solid:liquid ratios.[75] Solid loading significantly affected the total OH groups for pine bark lignin and oak bark lignin. At higher solid loading (from 1:20 to 1:10), more condensation (M_w increases) of lignin fragments was observed, accompanied by a decrease in the amount of OH groups due to the release of C_γ side chains.[111]

3.3.4. Combinatorial Severity Factors

In addition to individual observations of process temperature and process time, combinatorial parameters are often used to describe the process intensity in a single variable as a function of temperature and time. This is for example important when comparing heating processes and temperature holding times of different organosolv systems with different heating dynamics. The H-factor is calculated as the time integral of the cooking curve which depends on the temperature, and is usually used to maximize yields in the organosolv process by means of a statistical experimental design.[112–114] Another possibility is the introduction of a severity parameter. This allows the effect of different process parameters such as acid concentration, process temperature and time to be combined in one factor, the combinatorial severity factor (CSF).[115] Based on the H-factor model:

$$R_0 = \mathrm{t} \times \exp\left(\frac{\mathrm{T(t)} - 100}{14.75}\right) \tag{1}$$

$$\mathrm{CSF} = \log_{10} R_0 - \mathrm{pH} \tag{2}$$

The severity factor has its origin in the optimization of delignification, which is related to the extraction of cellulose, which largely goes hand in hand with lignin extraction.[116,117] Many works that have studied the influence of an increasing process severity on the structure of lignin have been able to determine the reduction of lignin's molecular weight, an increase in the concentration of phenolic OH groups, and dehydration reactions on the side chain of the lignin or an increased acidolysis of the β—aryl—ether bonds.[33,81,118]

These observations are of course related to the influence of process temperature, process time and catalyst concentration since the CSF is a combination of all these factors. ElHage et al. confirmed this trend with the variation of the severity factor during the isolation of lignin from *Miscanthus* × *giganteus*.[119] With increasing CSF (from 1.75 to 2.93), they found a decrease in M_w

and aliphatic OH group content, and an increase in phenolic OH groups. Furthermore, they demonstrated the presence of carbonyl groups using FT-IR spectra for a CSF >2.8. Accordingly, the formation of a carbonyl signal is indicative of β—aryl—ether cleavage and the corresponding formation of a Hibbert ketone or aldehyde group.

3.4. Influence of Pretreatments on the Organosolv Process—Autohydrolysis

One of the most used pre-treatment methods is the autohydrolysis (AH) of biomass prior to the organosolv process. It is performed by mixing the biomass with water and optionally with a catalyst and cooking either under reflux or in a pressure reactor. Time and temperature may vary over a broad range from 23 to 480 min and 150 to 200 °C, as seen in Table 3. Afterwards, the autohydrolyzed biomass is obtained by filtration, dried, and further subjected to organosolv delignification. Many studies use the autohydrolysis to extract hemicelluloses in a first step, which facilitates the delignification and thus leads to a higher lignin yield. But the yield is not the only parameter that can be influenced by this kind of pre-treatment: also, the structure of the lignin, including its molar mass, S/G ratio and functional group content is altered. Most studies examining these structural changes compare the organosolv lignins obtained from untreated biomass versus autohydrolyzed biomass using an identical organosolv process; this finding is summarized in Table 3.

There are no overall trends that can be observed when the same organosolv process is used for pre-treated and untreated biomasses. Solely the aliphatic OH groups seem to decrease when an autohydrolysis step is applied. One possible explanation for that might be a lower content of impurities like hemicelluloses, which possess many aliphatic hydroxyl groups. When comparing the purity of organosolv lignins with and without a prior autohydrolysis step, the autohydrolyzed ones show a higher purity.[67,121,122] In contrast, the phenolic OH groups increase in most cases with the pre-treatment, but there are also two studies identifying a slightly lower phenolic OH content. One of them, the work of Zhu et al., is in addition the only one that observed a decrease in the S/G ratio with the autohydrolyzed biomass, while in all other cases an increase was noted. When comparing the molar masses, also no trend is observable, neither for M_n and M_w nor for PDI. As already discussed in chapter 3.1, the process temperature plays an important role when depolymerization and condensation reactions compete. In the different studies listed in Table 3, the temperatures vary a lot, which makes it is difficult to compare them. Moreover, the autohydrolysis step is again the combination of many parameters like an additional treatment time and temperature on top of the organosolv process, as well as the effect of different catalysts. Ibrahim et al. examined the influence of temperature, time and catalyst (H_2SO_4) during AH:[67] with higher severity of the pre-treatment, the PDI decreases while the phenolic OH and carboxylic acid group contents increase. In another study, Ibrahim et al. investigated the effect of different catalysts in the autohydrolysis step.[123] They used sulfuric, phosphoric and oxalic acid, respectively, and found that regardless of the acid used, M_n and M_w were smaller than without catalyst, while the PDI showed no trend. Moreover, also the phenolic OH and carboxylic acid content, again, increased with use of acids. Grzybek et al. studied an autohydrolysis step with 3 % Na_2SO_3 at 90 °C prior to the organosolv delignification.[126] They examined three different biomasses using the same autohydrolysis and organosolv process, with no consistent trends for the molecular weight or the PDI. This leads to the conclusion, similar to section 3.1, that the optimal conditions for the organosolv process, but also for the autohydrolysis pre-treatment, vary from biomass to biomass and need to be examined for each individually. It has already been reported, that G units possess a higher tendency for recondensation reactions,[127,128] which should be considered when choosing the pre-treatment conditions.

Another way to modify the organosolv lignin structure can be the addition of organic scavengers like *m*-cresol, *p*-nitrophenol, 2-naphthol, etc., as shown in **Table 4**. These substances act as carbenium ion scavengers, that can inhibit recondensation reactions of lignins during hydrolysis, and thus improve the lignin extractability.[127] The proposed mechanism is shown in **Figure 9**.

Here, some trends are in fact observable: when an organic scavenger is used, M_w as well as the PDI decrease compared to the process without the scavenger. This can be explained by the inhibition of recondensation reactions, as shown in Figure 9: with the addition of the different organic scavengers path B is favored, leading to smaller molar masses than for path A. The S/G-ratio is only measured in two of the studies, but both show either a constant ratio or an increase.

Regarding the functional groups, all studies determined an increase in the phenolic OH group content when the organic scavengers were added, which is not unexpected, as these molecules all possess phenolic OH groups: when they are then incorporated into the lignin's structure, they contribute to the phenol content. The aliphatic OH content again decreases in most cases, as well as the carboxylic acid and methoxy group content.

4. Conclusion

Variation of the acidic ethanosolv process parameters discussed here (especially temperature and time) has a significant effect on the structural composition of the derived lignins. It has been shown that these parameters influence the ratio of the competing depolymerization and condensation reactions and thus the resulting lignin structure. This trend can even be confirmed independently of the type of lignocellulosic biomass that was used in the original publications. In addition, the trends derived from experimental data are supported by computational calculations such as bond dissociation energies. Direct correlations were found between process temperature and time with the molecular weight of lignin and its content of phenolic and aliphatic hydroxyl groups. With increasing temperature, the molecular weight and concentration of aliphatic hydroxyl groups decrease, while the concentration of phenolic hydroxyl groups increases. A similar development is indicated for longer process times and the addition of an autohydrolysis step prior to organosolv pulping, but this is not entirely consistent when molecular weight is considered. Yet, when an organic scavenger is used for the autohydrolysis, M_w as well as the PDI decrease compared to the process without the scavenger, while the phenolic OH content increases. The data set is not large enough to determine further trends for other process parameters (like particle size, solid:liquid ratio, etc.), but

Table 4. Autohydrolysis (AH) and organosolv (OS) process using organic scavengers.

Biomass (particle size)	Autohydrolysis parameters	Organic scavenger (used in AH/OS)	Organosolv parameters	M_n [Da]	M_w [Da]	PDI [-]	S/G-Ratio [-]	Aliph. OH	Phen. OH	COOH [mmol g^{-1}]	OCH_3 [amount/Ar]	Refs.
Oil palm fronds (1– 3 mm)	150 °C, 360 min, 1:9	–	190 °C, 60 min, 65% aq. EtOH with 0.5% (w/w) H_2SO_4, 1:8	1581	4023	2.54		0.36[a)]	0.45[a)]		1.74	[129, 130]
		p-nitrophenol (AH)		1381	2876	2.08		0.31[a)]	0.48[a)]		1.62	
		m-cresol (AH)		1212	2537	2.09		0.29[a)]	0.49[a)]		1.57	
Oil palm fronds (2– 4 mm)	150 °C, 360 min, 1:8	–	190 °C, 60 min, 65% aq. EtOH with 0.5% (w/w) of 4 N H_2SO_4, 1:9	411	822	2.00	2.64	0.61[a)]	0.50[a)]		2.42	[131]
		p-hydroxy-acetophenone (AH)		460	784	1.70	1.96	0.64[a)]	0.59[a)]		1.85	
Oil palm fronds (1– 3 mm for AH, 200 µm for OS)	150 °C, 480 min, 1:9, $s_0 \approx 4.1$	–	190 °C, 60 min, 65% aq. EtOH with 0.5% (w/w) H_2SO_4, 1:8, $s_0 \approx 2.5$	2372	5151	2.17		1.49[b)]	1.35 (0.69 S, 0.45 G, 0.21 H)[b)]	0.07		[132]
		2-naphthol (AH)		1647	3093	1.88		1.42[b)]	1.5 (0.79 S, 0.47 G, 0.24 H)[b)]	0.05		
		1,8-dihydroxy-anthraquinone (AH)		1888	3624	1.92		1.08[b)]	1.49 (0.74 S, 0.46 G, 0.29 H)[b)]	0.01		
Masson pine (< 20 mesh)	–	–	180 °C, 60 min, 75% aq. EtOH with 2% H_2SO_4, 1:10	1143	3098	2.71	0.18	2.30[b)]	2.44[b)]	0.14		[133]
		2-naphthol (OS)		681	1802	2.65	0.18	2.02[b)]	2.65[b)]	0.14		
Poplar (< 20 mesh)		–		883	1935	2.19	1.04	1.65[b)]	2.76[b)]	0.09		
		2-naphthol (OS)		577	1335	2.31	0.92	1.54[b)]	2.84[b)]	0.08		

[a)] in Amount per Ar; [b)] in mmol g^{-1}.

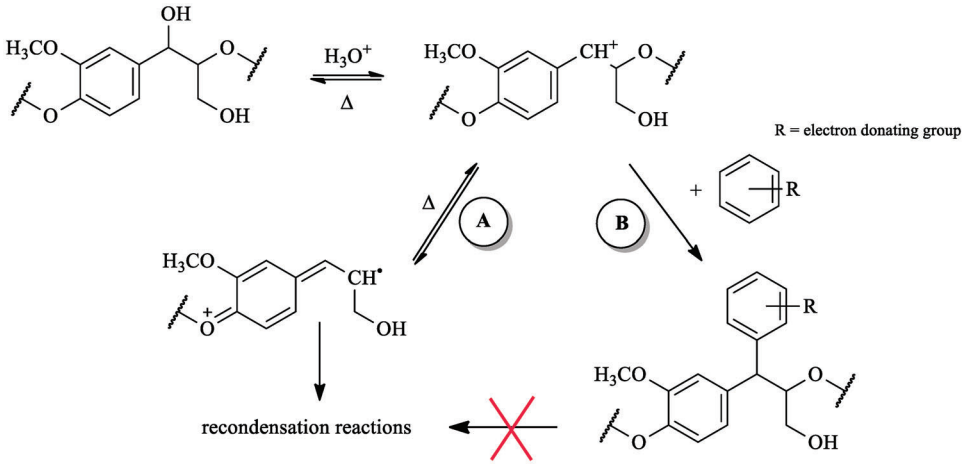

Figure 9. Scavenging effect of different aromatics. Adapted with permission.[127] Copyrights 2013, Elsevier.

some influences could be specified and can often be attributed to the ratio of depolymerization versus condensation reactions.

With the additional knowledge gained from this review, ethanol-organosolv lignins can be isolated more specifically for the desired application using simple process engineering methods. For example, increasing the temperature could increase the amount of phenolic hydroxyl groups, which can possibly be used to directly influence the antioxidant capacity, as this property positively correlates with the phenol content. Thus, a tailor-made isolation for the desired application seems possible.

Acknowledgements

Financial support was given by the BMBF (grant no. 13FH102PX8) and EFRE/NRW (grant no. EFRE 0500035). J.R. gratefully acknowledges a scholarship given by the Graduate Institute of the Bonn-Rhein-Sieg University of Applied Sciences.

Open access funding enabled and organized by Projekt DEAL.

Conflict of Interest

The authors declare no conflict of interest.

Keywords

acidic ethanosolv, autohydrolysis, condensation, depolymerization, lignin structure analysis, organosolv lignin, process parameters

Received: March 15, 2023
Revised: April 18, 2023
Published online: May 12, 2023

[1] S. Mariappan, A. D. Raj, S. Kumar, U. Chatterjee, in *Ecological Footprints of Climate Change: Adaptive Approaches and Sustainability* (Eds: U. Chatterjee, A. O. Akanwa, S. Kumar, S. K. Singh, A. D. Roy), Springer International Publishing, Cham, Switzerland **2022**, p. 63.
[2] S. Yu, L. Wang, Q. Li, Y. Zhang, H. Zhou, *Mater. Today Sustainability* **2022**, *19*, 100209.
[3] E. Jozami, F. D. Mele, R. Piastrellini, B. M. Civit, S. R. Feldman, *Energy* **2022**, *254*, 124215.
[4] M. V. Kulikova, A. Y. Krylova, F. G. Zhagfarov, K. O. Krysanova, A. L. Lapidus, *Chem. Technol. Fuels Oils* **2022**, *58*, 320.
[5] S. C. Rabelo, P. Y. S. Nakasu, E. Scopel, M. F. Araújo, L. H. Cardoso, A. C. Da Costa, *Bioresour. Technol.* **2023**, *369*, 128331.
[6] X. Lv, J. Lin, L. Luo, D. Zhang, S. Lei, W. Xiao, Y. Xu, Y. Gong, Z. Liu, *Bioresour. Technol.* **2018**, *249*, 226.
[7] J. C. Santana, A. K. Souza Abud, A. Wisniewski, S. Navickiene, L. P. C. Romão, *Biomass Bioenergy* **2020**, *133*, 105454.
[8] Z. Li, D. Xie, W. Zhu, H. Wang, T. Ouyang, J. Sun, Y. Wu, F. Cheng, *iScience* **2023**, *26*, 105771.
[9] S. Ahmad, V. V. Pathak, R. Kothari, R. P. Singh, *Biofuels* **2018**, *9*, 575.
[10] V. K. Garlapati, A. K. Chandel, S. P. J Kumar, S. Sharma, S. Sevda, A. P. Ingle, D. Pant, *Renewable Sustainable Energy Rev.* **2020**, *130*, 109977.
[11] B. M. Upton, A. M. Kasko, *Chem. Rev.* **2016**, *116*, 2275.
[12] R. Süss, G. Aufischer, L. Zeilerbauer, B. Kamm, G. Meissner, H. Spod, C. Paulik, *Catal. Commun.* **2022**, *170*, 106503.
[13] R. Süss, B. Kamm, D. Arnezeder, L. Zeilerbauer, C. Paulik, *Can. J. Chem. Eng.* **2022**, *100*, S38.
[14] N. L. Radhika, S. Sachdeva, M. Kumar, *Fuel* **2022**, *312*, 122935.
[15] H. Yu, B. Wang, Y. Wang, E. Xu, R. Wang, S. Wu, W. Wu, B. Ji, X. Feng, H. Xu, Y. Zhong, Z. Mao, *ACS Sustainable Chem. Eng.* **2023**, *11*, 4082.
[16] Anushikha, K. K. G, *Biomass Convers. Biorefin.* **2023**, https://doi.org/10.1007/s13399-022-03707-3
[17] R. Yadav, O. Zabihi, S. Fakhrhoseini, H. A. Nazarloo, A. Kiziltas, P. Blanchard, M. Naebe, *Composites, Part B* **2023**, *255*, 110613.
[18] P. Supchocksoonthorn, N. Hrimchum, T. Budsrirak, S. Intaraprasit, N. Thongsai, D. Aussawasathien, *Electrochim. Acta* **2023**, *437*, 141523.
[19] J. Gracia-Vitoria, S. C Gándara, E. Feghali, P. Ortiz, W. Eevers, K. S. Triantafyllidis, K. Vanbroekhoven, *Curr. Opin. Green Sustainable Chem.* **2023**, *40*, 100781.
[20] W. Li, L. Chai, B. Du, X. Chen, R.-C. Sun, *Sep. Purif. Technol.* **2023**, *306*, 122644.
[21] A. Naseer, A. Jamshaid, A. Hamid, N. Muhammad, M. Ghauri, J. Iqbal, S. Rafiq, S. Khuram, N. S. Shah, *Z. Phys. Chem.* **2019**, *233*, 315.
[22] M. Gericke, J. Bergrath, M. Schulze, T. Heinze, *Cellulose* **2022**, *29*, 3613.
[23] W. M. Moreira, P. V. V. Moreira, D. F. Dos Santos, M. L. Gimenes, M. G. A. Vieira, *Environ. Sci. Pollut. Res.* **2023**, *30*, 19564.

[24] D. Lebedeva, S. Hijmans, A. P. Mathew, E. Subbotina, J. S. M. Samec, *ACS Agric. Sci. Technol.* **2022**, *2*, 349.
[25] A. Lourenço, J. Gominho, *Lignin – Chemistry, Structure, and Application* (Eds: A. Sand, J. Tuteja), IntechOpen, London **2023**.
[26] J. A. Ferreira, M. J. Taherzadeh, *Bioresour. Technol.* **2020**, *299*, 122695.
[27] X. Lu, X. Gu, Y. Shi, *Int. J. Biol. Macromol.* **2022**, *210*, 716.
[28] M. N. Borand, F. Karaosmanoglu, *J. Renewable Sustainable Energy* **2018**, *10*, 033104.
[29] E. I. Evstigneyev, S. M. Shevchenko, *Wood Sci. Technol.* **2020**, *54*, 787.
[30] A. Romaní, C. M. Rocha, M. Michelin, L. Domingues, J. A. Teixeira, in *Current Developments in Biotechnology and Bioengineering: Bioprocesses, Bioreactors and Controls* (Eds: C. Larroche, M. Sanroman, G. Du, A. Pandey), Elsevier, Amsterdam **2020**, p. 383.
[31] D. Chettri, S. Ahmed, A. A. Malik, A. K. Verma, *BioEnergy Res.* **2023**, https://doi.org/10.1007/s12155-022-10561-8
[32] J. Xu, C. Li, L. Dai, C. Xu, Y. Zhong, F. Yu, C. Si, *ChemSusChem* **2020**, *13*, 4284.
[33] Z. Zhang, M. D. Harrison, D. W. Rackemann, W. O. S. Doherty, I. M. O'hara, *Green Chem.* **2016**, *18*, 360.
[34] Z. Zhou, F. Lei, P. Li, J. Jiang, *Biotechnol. Bioeng.* **2018**, *115*, 2683.
[35] W. Schutyser, T. Renders, S. Van Den Bosch, S.-F. Koelewijn, G. T. Beckham, B. F. Sels, *Chem. Soc. Rev.* **2018**, *47*, 852.
[36] N. Brosse, M. H. Hussin, A. A. Rahim, *Adv. Biochem. Eng./Biotechnol.* **2019**, *166*, 153.
[37] M. Källström, N. Meine, C. Farès, R. Rinaldi, F. Schüth, *Green Chem.* **2014**, *16*, 2454.
[38] Y. Barrière, J. Ralph, V. Méchin, S. Guillaumie, J. H. Grabber, O. Argillier, B. Chabbert, C. Lapierre, *C. R. Biol.* **2004**, *327*, 847.
[39] C. Heitner, D. Dimmel, J. Schmidt, *Lignin and Lignans*, CRC Press, Boca Raton, FL **2016**.
[40] J. M. Younker, A. Beste, A. C. Buchanan, *Chem. Phys. Lett.* **2012**, *545*, 100.
[41] E. Jasiukaitytė-Grojzdek, M. Huš, M. Grilc, B. Likozar, *Sci. Rep.* **2020**, *10*, 11037.
[42] J. Rumpf, X. T. Do, R. Burger, Y. B. Monakhova, M. Schulze, *Biomacromolecules* **2020**, *21*, 1929.
[43] J.-L. Wen, B.-L. Xue, S.-L. Sun, R.-C. Sun, *J. Chem. Technol. Biotechnol.* **2013**, *88*, 1663.
[44] P. J. De Wild, W. J. J. Huijgen, H. J. Heeres, *J. Anal. Appl. Pyrolysis* **2012**, *93*, 95.
[45] X. Zhao, D. Liu, *Bioenergy Res.* **2013**, *6*, 436.
[46] J.-B. Huang, S.-B. Wu, H. Cheng, M. Lei, J.-J. Liang, H. Tong, *Ranliao Huaxue Xuebao* **2015**, *43*, 429.
[47] S. Kim, S. C. Chmely, M. R. Nimlos, Y. J. Bomble, T. D. Foust, R. S. Paton, G. T. Beckham, *J. Phys. Chem. Lett.* **2011**, *2*, 2846.
[48] M. R. Sturgeon, S. Kim, K. Lawrence, R. S. Paton, S. C. Chmely, M. Nimlos, T. D. Foust, G. T. Beckham, *ACS Sustainable Chem. Eng.* **2014**, *2*, 472.
[49] X. Mu, Z. Han, C. Liu, D. Zhang, *J. Phys. Chem. C* **2019**, *123*, 8640.
[50] T. Azad, J. D. Schuler, M. L. Auad, T. Elder, A. J. Adamczyk, *Energy Fuels* **2020**, *34*, 9709.
[51] R. Parthasarathi, R. A. Romero, A. Redondo, S. Gnanakaran, *J. Phys. Chem. Lett.* **2011**, *2*, 2660.
[52] C. W. Lahive, P. J. Deuss, C. S. Lancefield, Z. Sun, D. B. Cordes, C. M. Young, F. Tran, A. M. Z. Slawin, J. G. De Vries, P. C. J. Kamer, N. J. Westwood, K. Barta, *J. Am. Chem. Soc.* **2016**, *138*, 8900.
[53] F. P. Marques, A. S. Colares, M. N. Cavalcante, J. S. Almeida, D. Lomonaco, L. M. A. Silva, M. De Freitas Rosa, R. C. Leitão, *Ind. Eng. Chem. Res.* **2022**, *61*, 4058.
[54] D. S. Zijlstra, C. W. Lahive, C. A. Analbers, M. B. Figueirêdo, Z. Wang, C. S. Lancefield, P. J. Deuss, *ACS Sustainable Chem. Eng.* **2020**, *8*, 5119.
[55] R. Samuel, Y. Pu, B. Raman, A. J. Ragauskas, *Appl. Biochem. Biotechnol.* **2010**, *162*, 62.
[56] S. Chow, P. R. Steiner, *J. Appl. Polym. Sci.* **1979**, *23*, 1973.
[57] E. Kumpinsky, *Ind. Eng. Chem. Res.* **1995**, *34*, 3096.
[58] P. J. Deuss, K. Barta, *Coord. Chem. Rev.* **2016**, *306*, 510.
[59] A. Tolbert, H. Akinosho, R. Khunsupat, A. K. Naskar, A. J. Ragauskas, *Biofuels, Bioprod. Biorefin.* **2014**, *8*, 836.
[60] S. Baumberger, A. Abaecherli, M. Fasching, G. Gellerstedt, R. Gosselink, Bo Hortling, J. Li, B. Saake, E. De Jong, *Holzforschung* **2007**, *61*, 459.
[61] E. S. Esakkimuthu, N. Marlin, M.-C. Brochier-Salon, G. Mortha, *Appl. Chem.* **2022**, *2*, 30.
[62] T. Rashid, C. F. Kait, T. Murugesan, *Proc. Eng.* **2016**, *148*, 1312.
[63] P. Korntner, I. Sumerskii, M. Bacher, T. Rosenau, A. Potthast, *Holzforschung* **2015**, *69*, 807.
[64] C. Qu, S. Ogita, H. Kawamoto, T. Kishimoto, *Holzforschung* **2022**, *76*, 567.
[65] Q. Shen, Z. Fu, R. Li, Y. Wu, *J. Therm. Anal. Calorim.* **2021**, *146*, 1751.
[66] M. Bergs, X. T. Do, J. Rumpf, P. Kusch, Y. Monakhova, C. Konow, G. Völkering, R. Pude, M. Schulze, *RSC Adv.* **2020**, *10*, 10740.
[67] Q. Ibrahim, A. Kruse, *Bioresour. Technol. Rep.* **2020**, *11*, 100506.
[68] P. Giraudeau, *Magn. Reson. Chem.* **2014**, *52*, 259.
[69] F. Fardus-Reid, J. Warren, A. Le Gresley, *Anal. Methods* **2016**, *8*, 2013.
[70] M. Sette, H. Lange, C. Crestini, *Comput. Struct. Biotechnol. J.* **2013**, *6*, e201303016.
[71] S. D. Mansfield, H. Kim, F. Lu, J. Ralph, *Nat. Protoc.* **2012**, *7*, 1579.
[72] R. Burger, J. Rumpf, X. T. Do, Y. B. Monakhova, B. W. K. Diehl, M. Rehahn, M. Schulze, *ACS Omega* **2021**, *6*, 29516.
[73] M. L. T. M. Polizeli, A. C. S. Rizzatti, R. Monti, H. F. Terenzi, J. A. Jorge, D. S. Amorim, *Appl. Microbiol. Biotechnol.* **2005**, *67*, 577.
[74] W. J. J. Huijgen, G. Telysheva, A. Arshanitsa, R. J. A. Gosselink, P. J. De Wild, *Ind. Crops Prod.* **2014**, *59*, 85.
[75] Li-Y Liu, S. C. Patankar, R. P. Chandra, N. Sathitsuksanoh, J. N. Saddler, S. Renneckar, *ACS Sustainable Chem. Eng.* **2020**, *8*, 4745.
[76] X. Pan, J. F. Kadla, K. Ehara, N. Gilkes, J. N. Saddler, *J. Agric. Food Chem.* **2006**, *54*, 5806.
[77] A. Ovejero-Pérez, V. Rigual, J. C. Domínguez, M. V Alonso, M. Oliet, F. Rodriguez, *Int. J. Biol. Macromol.* **2022**, *197*, 131.
[78] J. R. Meyer, H. Li, J. Zhang, M. B. Foston, *ChemSusChem* **2020**, *13*, 4557.
[79] R. N. Nishide, J. H. Truong, M. M. Abu-Omar, *ACS Omega* **2021**, *6*, 8142.
[80] L. Yao, L. Xiong, C. G. Yoo, C. Dong, X. Meng, J. Dai, A. J. Ragauskas, C. Yang, J. Yu, H. Yang, X. Chen, *Sustainable Energy Fuels* **2020**, *4*, 5114.
[81] M. Hochegger, B. Cottyn-Boitte, L. Cézard, S. Schober, M. Mittelbach, *Int. J. Chem. Eng.* **2019**, *2019*, 1734507.
[82] Xi-C Cheng, X.-R. Guo, Z. Qin, X-De Wang, H.-M. Liu, Y.-L. Liu, *Int. J. Biol. Macromol.* **2020**, *164*, 4348.
[83] M. S. Yáñez, B. Matsuhiro, C. Nuñez, S. Pan, C. A. Hubbell, P. Sannigrahi, A. J. Ragauskas, *Polym. Degrad. Stab.* **2014**, *110*, 184.
[84] R. Rinaldi, R. Jastrzebski, M. T. Clough, J. Ralph, M. Kennema, P. C. A. Bruijnincx, B. M. Weckhuysen, *Angew. Chem., Int. Ed. Engl.* **2016**, *55*, 8164.
[85] X. Liu, F. P. Bouxin, J. Fan, V. L. Budarin, C. Hu, J. H. Clark, *ChemSusChem* **2020**, *13*, 4296.
[86] J. Tao, O. Hosseinaei, L. Delbeck, P. Kim, D. P. Harper, J. J. Bozell, T. G. Rials, N. Labbé, *RSC Adv.* **2016**, *6*, 79228.
[87] L. Yao, C. Chen, C. G. Yoo, X. Meng, Mi Li, Y. Pu, A. J. Ragauskas, C. Dong, H. Yang, *ACS Sustainable Chem. Eng.* **2018**, *6*, 14767.
[88] Y. Guo, J. Zhou, J. Wen, G. Sun, Y. Sun, *Ind. Crops Prod.* **2015**, *76*, 522.
[89] S. Bauer, H. Sorek, V. D. Mitchell, A. B. Ibáñez, D. E. Wemmer, *J. Agric. Food Chem.* **2012**, *60*, 8203.
[90] P. Paulsen Thoresen, H. Lange, C. Crestini, U. Rova, L. Matsakas, P. Christakopoulos, *ACS Omega* **2021**, *6*, 4374.

[91] J. Wildschut, A. T. Smit, J. H. Reith, W. J. J. Huijgen, *Bioresour. Technol.* **2013**, *135*, 58.
[92] P. Sannigrahi, A. J. Ragauskas, in *Aqueous Pretreatment of Plant Biomass for Biological and Chemical Conversion to Fuels and Chemicals* (Ed: C. E. Wyman), John Wiley & Sons, Ltd. Chichester, UK **2013**, p. 201.
[93] Li Shuai, B. Saha, *Green Chem.* **2017**, *19*, 3752.
[94] S. Constant, C. Basset, C. Dumas, F. Di Renzo, M. Robitzer, A. Barakat, F. Quignard, *Ind. Crops Prod.* **2015**, *65*, 180.
[95] P. Ferrini, R. Rinaldi, *Angew. Chem., Int. Ed. Engl.* **2014**, *53*, 8634.
[96] T. Leskinen, S. S. Kelley, D. S. Argyropoulos, *ACS Sustainable Chem. Eng.* **2015**, *3*, 1632.
[97] G. F. Zakis, *Functional Analysis of Lignins and Their Derivates*, TAPPI Press, Atlanta **1994**.
[98] T. Kleinert, K. V. Tayenthal, *Angew. Chem.* **1931**, *44*, 788.
[99] P. Bajpai, in *Biermann's Handbook of Pulp and Paper*, Elsevier, Amsterdam **2018**, p. 295.
[100] M. Mohan, K. Huang, V. R. Pidatala, B. A. Simmons, S. Singh, K. L. Sale, J. M. Gladden, *Green Chem.* **2022**, *24*, 1165.
[101] D. T. Balogh, A. A. S. Curvelo, R. A. M. C. De Groote, *Holzforschung* **1992**, *46*, 343.
[102] K. H. Kim, C. S. Kim, *Front. Energy Res.* **2018**, *6*, 92.
[103] P. Schulze, A. Seidel-Morgenstern, H. Lorenz, M. Leschinsky, G. Unkelbach, *Bioresour. Technol.* **2016**, *199*, 128.
[104] D. S. Zijlstra, C. A. Analbers, J. de Korte, E. Wilbers, P. J. Deuss, *Polymers* **2019**, *11*, 1913.
[105] M. Michelin, S. Liebentritt, A. A. Vicente, J. A. Teixeira, *Int. J. Biol. Macromol.* **2018**, *120*, 159.
[106] M. Hundt, K. Schnitzlein, M. G. Schnitzlein, *Bioresour. Technol.* **2013**, *136*, 672.
[107] X. Zhu, J. Sipilä, A. Potthast, T. Rosenau, M. Balakshin, *J. Agric. Food Chem.* **2023**, *71*, 580.
[108] I. Miranda, J. Gominho, I. Mirra, H. Pereira, *Ind. Crops Prod.* **2012**, *36*, 395.
[109] F. Carvalheiro, L. C. Duarte, F. Pires, V. Van-Dúnem, L. Sanfins, L. B. Roseiro, F. Gírio, *Energies* **2022**, *15*, 5654.
[110] F. D. C. Siacor, I. D. F. Tabanag, C. F. Y. Lobarbio, E. B. Toboada, *Sci. Technol. Asia* **2021**, *26*, 34.
[111] *Lignin: Historical, Biological, and Materials Perspectives* (Eds: W. G. Glasser, R. A. Northey, T. P. Schultz), American Chemical Society, Washington, DC **1999**.
[112] E. Araque, C. Parra, J. Freer, D. Contreras, J. Rodríguez, R. Mendonça, J. Baeza, *Enzyme Microb. Technol.* **2008**, *43*, 214.
[113] M. S. Yáñez, J. Rojas, J. Castro, A. Ragauskas, J. Baeza, J. Freer, *J. Chem. Technol. Biotechnol.* **2013**, *88*, 39.
[114] P. Vergara, M. Ladero, F. García-Ochoa, J. C. Villar, *Ind. Crops Prod.* **2018**, *124*, 856.
[115] N. Abatzoglou, E. Chornet, K. Belkacemi, R. P. Overend, *Chem. Eng. Sci.* **1992**, *47*, 1109.
[116] *Hydrothermal Processing in Biorefineries*, (Eds: H. A. Ruiz, M. H. Thomsen, H. L. Trajano), Springer International Publishing, Cham, Switzerland **2017**.
[117] C. E. De Farias Silva, A. Bertucco, *Bioenergy Res.* **2018**, *11*, 491.
[118] S.-K. Jang, Ho-Y Kim, H.-S. Jeong, J.-Y. Kim, H. Yeo, In-G Choi, *Renewable Energy* **2016**, *87*, 599.
[119] R. El Hage, N. Brosse, P. Sannigrahi, A. Ragauskas, *Polym. Degrad. Stab.* **2010**, *95*, 997.
[120] M.-Q. Zhu, J.-L. Wen, Y.-Q. Su, Q. Wei, R.-C. Sun, *Bioresour. Technol.* **2015**, *185*, 378.
[121] S. Saad, I. Dávila, F. Mannai, J. Labidi, Y. Moussaoui, *Biomass Conv. Bioref.* **2022**, 1.
[122] A. Morales, J. Labidi, P. Gullón, *Sustainable Mater. Technol.* **2022**, *33*, e00474.
[123] Q. Ibrahim, P. J. Arauzo, A. Kruse, *Renewable Energy* **2020**, *153*, 1479.
[124] P. Obama, G. Ricochon, L. Muniglia, N. Brosse, *Bioresour. Technol.* **2012**, *112*, 156.
[125] J.-L. Wen, S-Ni Sun, T-Qi Yuan, F. Xu, R.-C. Sun, *Bioresour. Technol.* **2013**, *150*, 278.
[126] J. Grzybek, T. Sepperer, A. Petutschnigg, T. Schnabel, *Materials* **2021**, *14*, 7774.
[127] Y. P. Timilsena, I. G. Audu, S. K. Rakshit, N. Brosse, *Biomass Bioenergy* **2013**, *52*, 151.
[128] T. Komatsu, T. Yokoyama, *J. Food Sci.* **2021**, *67*, 45.
[129] N. A. Sa'don, A. A. Rahim, M. H Hussin, *Int. J. Biol. Macromol.* **2017**, *98*, 701.
[130] N. A. Sa'don, A. A. Rahim, M. N. M. Ibrahim, N. Brosse, M. H Hussin, *Int. J. Biol. Macromol.* **2017**, *104*, 251.
[131] N. H. A. Latif, A. A. Rahim, N. Brosse, M. H Hussin, *Int. J. Biol. Macromol.* **2019**, *130*, 947.
[132] M. H Hussin, A. A. Rahim, M. N. Mohamad Ibrahim, N. Brosse, *Mater. Chem. Phys.* **2015**, *163*, 201.
[133] K. Wang, C. Yang, X. Xu, C. Lai, D. Zhang, Q. Yong, *Renewable Energy* **2022**, *200*, 767.

Jonas Bergrath works as a research associate at the Department of Applied Natural Sciences at the University of Applied Sciences Bonn-Rhein-Sieg and is a Ph.D. student at the University of Wuppertal. His research interests are the utilization of biogenic biomasses and the structure–property relationships of lignin. He received his M.Sc. degree in chemistry from the University of Wuppertal.

Jessica Rumpf is a doctoral researcher at the Bonn-Rhein-Sieg University of Applied Sciences and the University of Bonn (Germany). Her research focuses on lignins from low-input crops, their structure elucidation, and the analysis of their antioxidant properties for potential applications as antioxidant additives. She received both her M.Sc. degree in analytical chemistry and quality assurance and her B.Sc. degree in chemistry with materials science from the Bonn-Rhein-Sieg University of Applied Sciences.

Margit Schulze is professor for industrial organic chemistry and polymers at the Hochschule Bonn-Rhein-Sieg in Rheinbach (Germany) and Privatdozentin at the Agricultural Faculty of the Rheinische Friedrich-Wilhelms-University Bonn (Germany). In 1991, she obtained her Ph.D. in organic chemistry from the Technical University Merseburg (Germany). After post-doctoral stays at the Max-Planck-Institute for Polymer Research Mainz (Germany), Fraunhofer-Institute for Material Research Teltow (Germany) and Royal Institute of Technology (KTH) Stockholm (Sweden) she was head of the Industrial Oils Lab at Evonik RohMax Additives GmbH Darmstadt (Germany). Her research interest is focused on biomass and related waste exploitation for future material design.

